Equilibrium Isotherm, Kinetic, and Thermodynamic Studies of Divalent Cation Adsorption onto *Calamus gracilis* Sawdust-Based Activated Carbon

Ganiyu Abimbola Adebisi, Zaira Zaman Chowdhury,* Sharifah Bee Abd Hamid, and Eaqub Ali

Activated carbon (RSAC) was prepared using the two steps of hydrothermal carbonization (HTC) and chemical activation from the sawdust of *Calamus gracilis*, commonly known as Rattan (RS). The HTC process was carried out using a Teflon-lined autoclave to produce hydrochar, followed by chemical activation using phosphoric acid (H_3PO_4). The highest removal percentage obtained for lead, Pb(II), and zinc, Zn(II), cations were 86.71% and 64.26%, respectively, using the initial adsorbate concentration of 350 mg/L at 30 °C. These values strongly indicated the promising adsorption potential of the newly prepared hydrochar-based activated carbon (RSAC) for the better management of industrial wastewater and effluents. The analysis of the equilibrium sorption data revealed that these adsorptions followed the Langmuir isotherm model and the pseudo-second order kinetic model. The adsorption process was endothermic and spontaneous. The prepared carbon (RSCAC) showed enhanced surface area with porous texture, which could effectively aid for elimination of Pb(II) and Zn(II) cations from waste water.

Keywords: Hydrochar; Kinetics; Langmuir monolayer adsorption capacity; Hydrothermal carbonization; Isotherm model; Thermodynamics

*Contact information: Nanotechnology & Catalysis Research Centre (NANOCAT), University of Malaya, Institute of Post Graduate Studies, 50603 Kuala Lumpur, Malaysia; *Corresponding authors: zaira.chowdhury76@gmail.com, dr.zaira.chowdhury@um.edu.my, sharifahbee@um.edu.my*

INTRODUCTION

The global demand for the abatement of environmental pollution calls for innovative approaches to the treatment of waste water using cost-effective strategies. Heavy metals are usually discharged into bodies of water through industrial activities, a practice that ought to be eliminated given that these metals are highly toxic and constitute a health hazard when consumed beyond the permissible level. Among the heavy metal pollutants, divalent cations such as lead (Pb), copper (Cu), manganese (Mn), arsenic (AS), cadmium (Cd), and zinc (Zn) are considered priority pollutants (Abdel-Halim *et al.* 2003). The presence of lead (Pb) in water, even at very low concentrations, can lead to kidney, nervous system, and reproductive system damage in humans (Chowdhury *et al.* 2012b). According to the World Health Organization (WHO), the recommended maximum acceptable concentration of lead in drinking water is 0.1 to 0.05 mg/L (Zhang *et al.* 2005). Zinc is known to be discharged into waterways by industries, especially those that use galvanizing plants and municipal wastewater treatment plants or are involved in acid mine drainage or natural ores (Moreno-Barbosa *et al.* 2013). The consumption of zinc is essential for human health, but its presence above the tolerable

dose in food and feed plants is of great concern due to its toxicity at these levels (Wang *et al.* 2012). Zinc is a non-biodegradable metal that travels through the food chain by bioaccumulation. According to WHO, the maximum recommended tolerable concentration of Zn in drinking water is 5.0 mg/L (Hawari *et al.* 2009).

Metallic pollutants have been removed from wastewaters using various technologies including precipitation, ion exchange, membrane filtration, and reverse osmosis (Baccar *et al.* 2009). These methods have several disadvantages, including the requirements of expensive equipment and secondary treatment for produced sludge prior to its disposal. Due to these limitations, the need has arisen for a more environmentally friendly method that is at the same time cost-effective. Efforts have been therefore geared towards the use of adsorption processes. The use of adsorbents in the removal of heavy metals from wastewaters has not only been found to be superior to the other conventional methods, but has equally been found to be cost-effective, simple in design, easy to operate, and much more user-friendly. For this reason, activated carbons have been in use as adsorbents for quite a long time. However, the commercial activated carbons are relatively expensive. Some agricultural wastes have been already utilized for the preparation of activated carbon adsorbents, including solid wastes (Al-Othman *et al*. 2011), coconut shell (Amuda *et al.* 2007), kenaf fiber (Chowdhury *et al.* 2012a), mangosteen fruit shell (Chowdhury *et al.* 2012b), bamboo culms (Ekebafe *et al.* 2012), oil palm empty fruit bunch (Foo and Hameed 2011), coconut shell (Gratuito *et al.* 2008), rattan sawdust (Hameed *et al.* 2007), and many others.

The hydrochar obtained from hydrothermal carbonization (HTC) can offer an innovative kind of precursor to prepare activated carbon (Adebesi *et al.* 2016). The physiochemical properties of HTC char resemble those of peat and lignite-, the characteristics of which can be modified using a suitable activation technique to obtain functional activated carbon for versatile applications (Hao *et al.* 2014). HTC char is easy to pelletize and does not involve the flow of gas (Amaya *et al.* 2007). Furthermore, the process can be carried out using water as 'green catalyst'. This makes the process economically viable. Depending on preparation conditions, lignocellulosic biomass can be converted to hydrochar having unique morphological structures (Titirici *et al.* 2008). After activation of HTC char at higher temperature, the aromaticity increases substantially (Falco *et al.* 2013). However, no studies have been reported on the production of adsorbents from rattan sawdust (RS) by means of hydrothermal treatment followed by phosphoric acid (H_3PO_4) activation and its application for heavy metals adsorption. Equilibrium kinetics, isotherm, and thermodynamic studies were conducted on the adsorption of Pb^{2+} and Zn^{2+} ions. The experimental data was analyzed using Langmuir, Freundlich, and Temkin isotherm models. The thermodynamic characterization of the system was determined using Gibb's free energy ($\Delta G°$), enthalpy ($\Delta H°$), and entropy ($\Delta S°$) values.

EXPERIMENTAL

Materials

Preparation of feedstock (RS)

Rattan core samples were collected from the Federal School of Agriculture, Akure, Nigeria. They were mechanically cut into small sizes and thoroughly washed in water to rid them of mud, dust, and other forms of dirt. They were then sun-dried for 4

weeks and finally oven-dried at 105 °C for 6 h. The precursor, once prepared, was packed in a plastic container, tightly covered, and labeled accordingly. $Pb(NO_3)_2.2H_2O$ and $Zn(NO_3)_2 \cdot 6H_2O$ having purity 99.98% were purchased from Sigma Aldrich (Irvine, UK). The chemicals used here were analytical reagent grade.

Preparation of hydrochar (RSC)

To prepare hydrochar, 5.0 g of residue was mixed with 50 mL of deionized water and stirred until it was homogeneously mixed. The sample was transferred into a Teflon-lined autoclave (100 mL) and carbonized for 12 h at 220 °C. The resulting char sample (RSC) was washed several times with deionized water until a neutral pH was obtained. It was dried at 105 °C for 6 h in an oven. The obtained RSC was not initially activated and was stored in air-tight containers for preliminary characterization studies.

Preparation of activated carbon (RSCAC)

Twenty grams of each sample was impregnated with 100 mL of H_3PO_4 (ratio 1:5, solid to liquid) and heated to 100 °C for 4 h, after which it was oven-dried at 90 °C for 24 h. The sample was then fed into a vessel of about 150 mm length and 40 mm diameter. The vessel was then transferred into the calcination furnace (Bamstead/Thermolyne 48000) that was fitted with a temperature knob to regulate the temperature. The vessel was also connected to nitrogen gas cylinder, and the pyrolysis of the sample was carried out using a continuous nitrogen gas flow of 100 mL/min. The carbonization was carried out at varying temperatures and times depending on the experimental design matrix using Design of Expert software, version 7. For carbonization, a regulated holding time of 2.04 h, a temperature 657.65 ^oC and an acid concentration for impregnation 40.54% were used as optimum conditions. The heating rate was kept constant at 5 ^oC/min. After carbonization was finished, the sample was allowed to cool to room temperature under an inert atmosphere and was then raked from the vessel. The sample was then washed with hot deionized water to remove any residual chemical agents until the pH became neutral and then dried at 65 °C for 12 h. This was then stored for the characterization, kinetics, and thermodynamics analyses, accordingly.

Methods

Characterization

The investigation of the surface porosity of the prepared activated carbons was carried out using a surface area analyzer (ASAP 2020 V4.01 model) based on the nitrogen adsorption-desorption isotherm at 77.313 K. The BET model was applied to fit the nitrogen adsorption isotherm with the surface area of the evaluated sorbent (Vernersson *et al.* 2002). The total pore volume was calculated using the total volume of N_2 adsorbed at a relative pressure of 0.995. In order to overcome the problem usually encountered when the linear form of the Dubinin-Radushkevich (DR) equation is used, a more generalized equation known as the Dubinin-Astakhov (DA) equation was employed in calculating the micro-pore surface area and the volume.

The proximate analysis of the starting raw materials (RS), hydro-char (RSC), and the activated carbons (RSCAC) prepared under optimum conditions were subjected to thermo-gravimetric analysis (TGA). The parameters analyzed include moisture, volatile matter, and fixed carbon and ash contents. The TGA analysis provided the opportunity to study the pyrolysis behavior of the samples, biochar, and the activated carbons. The moisture content was determined using the oven-drying test method, while the ash

content was determined by subjecting the samples to heating for 8 h at 650 °C until a consistent mass was obtained. The fixed carbon was estimated by the difference, in accordance with Durán-Valle *et al*. (2005), as follows:

Fixed carbon (%) = 100 – (moisture % + ash, % + volatile matter %). (1)

A CHNS analyzer was used in carrying out the elemental analysis. However, the percentage oxygen present was evaluated by the difference as follows:

Oxygen (%) = 100 – (C, % + H, % + N, % + S, %) (2)

The surface morphological changes in the RS, RSC, and RSCAC were characterized using field emission scanning electron microscopy (FE-SEM; model SUPRA 35VP, Zeiss, Germany, UK).

Equilibrium Isotherm Studies

The sorption of the adsorbates onto the adsorbents was studied through batch adsorption studies. The variations in the uptake levels of Pb^{2+} and Zn^{2+} ions with contact time were determined for each of the adsorbent. This was required in order to establish the equilibrium time (*i.e.*, the time for the adsorbent to reach the sorption equilibrium). To accomplish this, 0.2 g of each of the adsorbent were dispersed in 50 mL of each of the initial concentrations of 150, 200, 250, 300, and 350 mg/L solutions in well-stoppered plastic containers. The mixture was then thoroughly agitated at room temperature (30 °C) using a water bath shaker set at 150 rpm. At the end of the contact time, the mixture was filtered, and the residual concentration of the Pb^{2+} or Zn^{2+} ions (whatever the case may be) in the filtrate was determined by means of ICP (APHA 3125B, 20th edition, 1998). The amount of Pb^{2+} or Zn^{2+} adsorbed at equilibrium (q_e) was calculated from the following Eq. 1 (Chowdhury *et al.* 2011a,b, 2015),

$$q_e = \frac{(C_0 - C_e)V}{W} \quad (3)$$

where q_e represents the amount of ions adsorbed at equilibrium (mg/g), C_0 is the initial concentration of the targeted cation (mg/L), C_e is the liquid-phase concentrations of metal ions at equilibrium conditions (mg/L), V is the volume of the single solute solution (L), and W is the mass of RSCAC used (g). All the adsorption experiments were triplicated, and the average values were used for calculation. To be able to explain the interaction between the adsorbate and the adsorbent during the adsorption process, adsorption isotherms were applied, as this was critical for the design of the adsorption process. The batch adsorption process was repeated at different temperatures for the isotherm generation. In the present study, Langmuir, Freundlich, and Temkin isotherms were applied using Eqs. 4, 5, and 6, respectively (Adebesi *et al*. 2016),

$$\frac{C_e}{q_e} = \frac{1}{q_{\max} \mathrm{K_L}} + \frac{1}{q_{\max}} C_e \quad (4)$$

where q_m (mg/g) is the maximum monolayer adsorption capacity of the prepared carbon sample (RSCAC), and K_L (L/mg) is Langmuir's constant (Langmuir 1918). Likewise,

$$\ln q_e = \ln K_f + \frac{1}{n} \ln C_e \quad (5)$$

where K_f is the affinity factor of the cations towards the carbon sample (RSCAC) (mg/g), and 1/n represents the intensity of the adsorption (Freundlich 1906). Data were also analyzed by,

$$q_e = \frac{RT}{b} \ln K_T + \frac{RT}{b} \ln C_e \quad (6)$$

where $RT/b = B$ denotes the Temkin constant (J/mol.K), which represents the heat of the sorption process, whereas the value of K_T reveals the equilibrium binding constant (L/g), R is the universal gas constant (8.314 J/mol·K), and $T°$ is the absolute solution temperature (K) (Temkin and Pyzhev 1940).

Adsorption Kinetics

In order to examine the adsorption kinetics process in this study, three kinetic models were used. These are the pseudo-first-order kinetic model, the pseudo-second-order kinetic model, and the Elovich equation model. Furthermore, the diffusion mechanism for the process was studied by using an intra-particle diffusion model. Batch kinetic assays were performed using precisely weighted amounts of RSCAC (0.2 g) with known volumes (50 mL) of Pb(II) and Zn(II) solution having concentration from 150 mg/L to 350 mg/L. The mixture was placed in a plastic container and shaken by a shaker submerged in a water bath to control the temperature. After a predetermined time interval, the solution was taken out and filtered, and its concentration was determined using ICP (APHA 3125B, 20th edition, 1998). In an effort to study the effect which the solution pH exert on the adsorption of Pb(II) and Zn(II) ions onto BEFBAC and RSAC, the solution initial pH was varied between 2 to 14 while other adsorption process conditions were kept constant at T = 30 °C, time, t = 210 min, adsorbate initial concentration = 350 mg/L, and adsorbent dosage = 0.2 g.

Desorption Studies

In this study, regeneration analysis was carried out with 1 M solutions of hydrochloric acid (HCl), sulphuric acid (H_2SO_4), nitric acid (HNO_3), and deionized water. The adsorbent, after the adsorption process had been completed, was removed by filtration and transferred into stoppered containers, while 50 mL of each of the solutions was added and shaken at room temperature for 210 min using a water shaker (adsorption equilibrium time) and the initial concentration of 350 mg/L. The adsorbent was then removed and filtered. The concentration of lead and zinc in the aqueous solutions (filtrate) was then determined using the ICP method. Finally, the recovery efficiency (RE) of the adsorbent for the metal ions was calculated using the following equation,

$$\text{Recovery Efficiency, RE (\%)} = \frac{C_e(des)}{C_0 - C_e(des)} x \frac{100}{1} \frac{\text{Ce(des)}}{\text{Co-Ce(ads)}} \text{X} \frac{100}{1} \quad (7)$$

where C_o is the initial concentration of the adsorbate, C_e (ads) is the final concentration of adsorbate after adsorption, and C_e (des) is the final concentration of adsorbate after desorption.

RESULTS AND DISCUSSION

Characterization

The microscopic examination of the precursor, hydro-char, and the corresponding activated carbon were examined using a field emission scanning electron microscope (FE-SEM). After hydrothermal carbonization, the raw biomass was incompletely carbonized to yield brown hydrochar. As could be seen from the micrographs, the surface texture of the precursor (Fig. 1a) was very rough and covered with some materials that appeared to be uneven and undulating. The surface was comparatively clean and smooth after the hydrothermal carbonization. Some small particles were deposited over the surface of the hydrochar (Fig. 1b). After hydrothermal carbonization, the lignin was partially degraded (Falco *et al.* 2013). The internal surface area of the biomass sample (RS) was increased after the removal of lignin and minor substances like pectin and wax. Due to the shielding effect of the lignin, the cellulose and hemicellulose present inside the biomass matrix were not able to make contact with the surrounding hydrothermal environment; consequently, they could not be processed completely under the mild conditions used for hydrothermal carbonization (HTC).

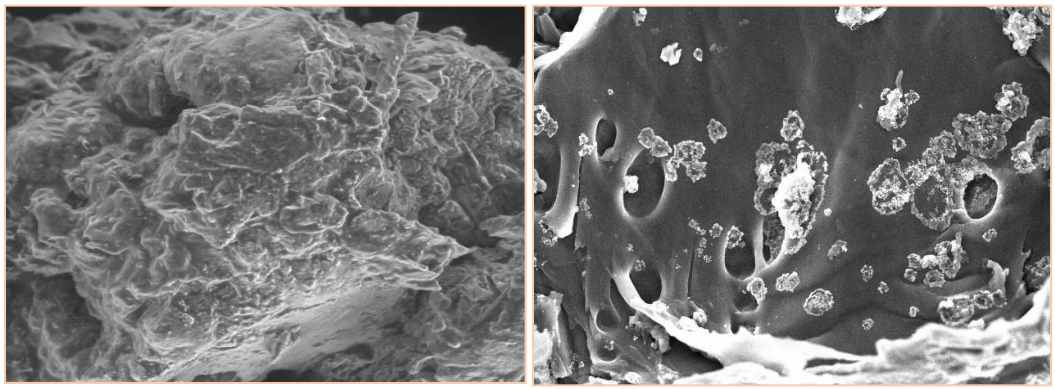

(a) RS (b) RSC

(c) RSCAC

Fig. 1. SEM micrographs of (a) RS, (b) RSC, and (c) RSAC

After the HTC process, the formation of some pores became noticeable on the surface of the hydro-char (Fig. 1b). After chemical activation with phosphoric acid, the pores became very clear, as can be seen from Fig. 1c. This result displayed that a radical

morphological change had occurred during the activation process and that the appearance of the final activated carbon sample retained no memory of the structure of the starting biomass (RS). Similar results were previously reported for banana empty fruit bunch and eucalyptus wood-based hydrochars (Adebesi *et al*. 2016; Sevilla and Fuertes 2011).

The BET surface area, pore volume, and pore size distribution of the raw RS, RSC, and RSAC are listed in Table 1. The hydrochar sample had a higher surface area than the starting biomass, indicating partial carbonization. However, the surface area and pore volume were increased substantially after the activation process. The results obtained here were consistent with the FE-SEM analysis. The results indicated that the activated carbon (RSCAC) had a BET surface area of 1,151.23 m^2/g. Additionally, RSAC was equally found to show a high total pore volume of 0.95 cm^3/g. Both the BET and the pore volume obtained for the prepared activated carbon were higher than those obtained for watermelon shell (710 m^2/g, 0.263 cm^3/g) and walnut shell (789 m^2/g and 0.304 cm^3/g) (Moreno-Barbosa *et al.* 2013). The high BET surface area and pore volumes of the RSAC were greatly enhanced by the two steps (hydrothermal treatment and chemical activation with phosphoric acid) undertaken in this preparation process. The H_3PO_4 acid further initiated the dehydration process and carried out the depolymerization reaction successfully, attacking the basal structural sheets inside the hydrochar matrix (Adebisi *et al.* 2016, Fernandez *et al*. 2015). Thus, the resultant activated carbon showed enhanced pore volume and surface area.

Table 1. Physico-Chemical Characteristics of RS, RSC, and Activated RSCAC

Sample Properties	RS	RSC	RSCAC
BET surface area (m^2/g)	1.23	169.28	1151.23
Micropore surface area (m^2/g)	0.87	147.66	837.66
Total pore volume (cc/g)	0.11	0.19	0.95
Average pore diameter (°A)	1.01	2.70	38.91
BJH cumulative adsorption surface area (m^2/g)	1.05	134.23	865.05

The proximate components, in percentage, of the precursors, hydro-chars, and their corresponding activated carbons are presented in Table 2. The results showed that the precursors were rich in volatile matters but that their fixed carbon contents were also high enough to support their conversion into carbons. Moreover, the results indicated a significant drop in the volatile matter content after hydrothermal treatment and subsequent activation and carbonization. During this period, the fixed carbon contents of the hydro-char increased progressively due to the breakdown of the bonds and linkages of the molecules of the organic compounds upon exposure to heat.

Table 2. Proximate Analysis of RS, RSC, and Activated RSCAC

Sample	Proximate Content (%)			
	Moisture	Volatile Matter	Ash	Fixed Carbon*
RS	17.87	27.98	14.15	40.00
RSC	15.00	19.05	19.78	46.17
RSAC	8.62	9.74	21.98	59.66

Table 3 lists the final contents of starting biomass, hydrochar, and hydrochar activated carbon. The carbon content of the samples increased progressively after the hydrothermal carbonization and activation process. However, the hydrogen and oxygen contents showed decreasing trends after the consecutive treatments of carbonization and activation (Saqib *et al.* 2015). The decrease in H/O and O/C ratios became noticeable after activation and carbonization due to the decarboxylation reaction and the aromatization processes occurring during these processes (Liu and Guo 2015). The H_3PO_4 acid aided in the dehydration process, as exhibited by the declining trend in both the H/C and O/C ratios.

Table 3. Final Contents of RS, RSC, and Activated RSCAC

Final Analyses	RS	RSC	RSCAC
Carbon (%)	42.31	56.74	84.65
Hydrogen (%)	6.00	3.12	2.29
Nitrogen (%)	0.64	0.45	0.62
Oxygen (%)	49.50	37.70	11.66
Others (%)	2.55	1.00	0.78
H/C	0.142	0.055	0.027
O/C	1.170	0.664	0.138

Equilibrium Isotherm Studies

The adsorption isotherm represents the ratio of the distribution of the adsorption molecules between the liquid phase (adsorbate) and the solid phase (adsorbent) at equilibrium state (Moreno-Barbosa *et al.* 2013). It is always important to analyze the experimental data in terms of various adsorption isotherm models so as to be able to determine which of the models best describes the adsorption process. For the present work, the experimental data was subjected to the linear forms of three isotherm models: Langmuir, Freundlich, and Temkin isotherm models. The three models were compared on the basis of their fit to the data using the values of the various constants obtained, especially the closeness of their coefficients of determination (R^2) values to unity.

Table 4 shows the Langmuir, Freundlich, and Temkin isotherm model parameters and the coefficients of determination of the adsorption of Pb(II) and Zn(II) cations onto RSCAC at 30 °C, 60 °C, and 80 °C, respectively. From the Table, it can be observed that for Pb(II) cations, the maximum monolayer sorption capacity q_m (mg/g) increased progressively at the temperatures of 30, 60, and 80 °C, whereas for Zn(II) cations, it decreased slightly at 60 °C but increased substantially around 80 °C. Furthermore, the applicability of the Langmuir isotherm was evaluated using the separation factor, R_L, which is normally dimensionless and used to determine whether an adsorption system is favorable or otherwise (Moreno-Barbosa *et al.* 2013). The R_L values were calculated using the following equation:

$$R_L = \frac{1}{1 + K_L C_o} \quad (8)$$

where C_o is the initial metal ion concentration and K_L is the Langmuir constant.

The value of R_L obtained is an indication of the type of isotherm as well as of the nature of the adsorption process (Moreno-Barbosa *et al.* 2013). The Langmuir R_L value can be described as follows: $R_L > 1$ (unfavorable), $R_L = 1$ (linear), $0 < R_L < 1$ (favorable), and $R_L = 0$ (irreversible) (Chowdhury *et al*. 2012b).

Table 4. Langmuir, Freundlich, and Temkin Model Parameters at Different Temperatures

Pollutant	Temperature (°C)	Langmuir Isotherm				Freundlich Isotherm			Temkin Isotherm		
		q_{max} (mg/g)	K_L (L/mg)	R^2	R_L	K_F (mg/g)(L/mg)$^{1/n}$	1/n	R^2	B	K_T (L/mg)	R^2
Pb(II)	30	101.01	0.04	0.97	0.06	11.64	0.46	0.90	0.39	23.12	0.82
	60	133.33	0.03	0.93	0.08	8.74	0.59	0.95	0.28	30.83	0.89
	80	129.87	0.04	0.94	0.07	9.59	0.57	0.95	0.31	29.67	0.89
Zn(II)	30	96.25	0.03	0.96	0.09	14.05	0.29	0.79	0.69	12.48	0.81
	60	95.24	0.02	0.93	0.08	10.03	0.45	0.94	0.29	22.00	0.92
	80	99.01	0.03	0.93	0.08	9.98	0.46	0.94	0.29	23.04	0.93

In the present study, the values of R_L were 0.06, 0.08, and 0.07 for Pb(II) cations and 0.09, 0.08, and 0.08 for Zn(II) cations at temperatures 30, 60, and 80 °C, respectively. The values of R_L fell between 0 and 1, revealing that the adsorption process for both the cations was favorable. This further displayed that the adsorption process fitted satisfactorily into the Langmuir isotherm model.

The Freundlich isotherm model describes the heterogeneity of the surface in an adsorption process (Chowdhury *et al.* 2012b). In the Freundlich model, when the value of $1/n$ is very close to 0, this indicates that the process is becoming heterogeneous, while when $1/n$ is less than 1, it signifies a normal Langmuir isotherm, and when the value is greater than 1, it indicates cooperative adsorption. The values of $1/n$ were less than 1, indicating that the adsorption process satisfactorily fit into a normal Langmuir isotherm model for both the cations (Table 4).

The fitness of the Langmuir model with the experimental data could be due to the homogeneous distribution of active sites on the adsorbent surface. Therefore, the applicability of the Langmuir isotherm model in the adsorption process was an indication of the monolayer attachment of Pb(II) and Zn(II) ions on the surface of the adsorbent (RSAC) (Chigondo *et al.* 2013).

The Temkin isotherm signifies the occupation of the more energetic adsorption sites by the adsorbate, that is, the interaction between the adsorbate and the adsorbent (Chowdhury *et al.* 2012b). The values of R^2 obtained for the Temkin model at room temperature (30 °C) were 0.82 for Pb(II) and 0.81 for Zn(II) cations. This was far lower than the values obtained for the Langmuir model at the same temperature, which was an indication that the experimental data fit better with the Langmuir model than with the Freundlich or Temkin models.

Effect of Contact Time

The effect of contact time on the equilibrium sorption process for the prepared adsorbent of (RSAC) is illustrated by Fig. 2 (a) and (b) for the Pb(II) and Zn(II) cations, respectively. From the figures, it can be observed that the sorption level of the adsorbent increased with the initial increase in sorption time until 210 min but remained relatively constant afterwards.

The adsorption uptake also increased with the increasing concentration of the solution. This trend with higher concentration was persistent due to the larger mass transfer between the adsorbate and adsorbent materials, leading to more equilibrium uptake, results that were in agreement with our previous work studying the sorption of Cu(II) cations onto biochar (Abd Hamid *et al.* 2014).

This phenomenon was described earlier for the adsorption studies of Pb(II), Cd(II), and Ni(II) cations onto sawdust (Bulut and Tez 2007). Overall, the trend of the curve suggested that within 210 minutes, all the active sites had to have been saturated with the adsorbate metallic cation.

A similar trend had been observed by Khezami *et al.* (2012) and Chowdhury *et al.* (2012b). The point of the observed saturation corresponded to the maximum sorption limit of the adsorbent.

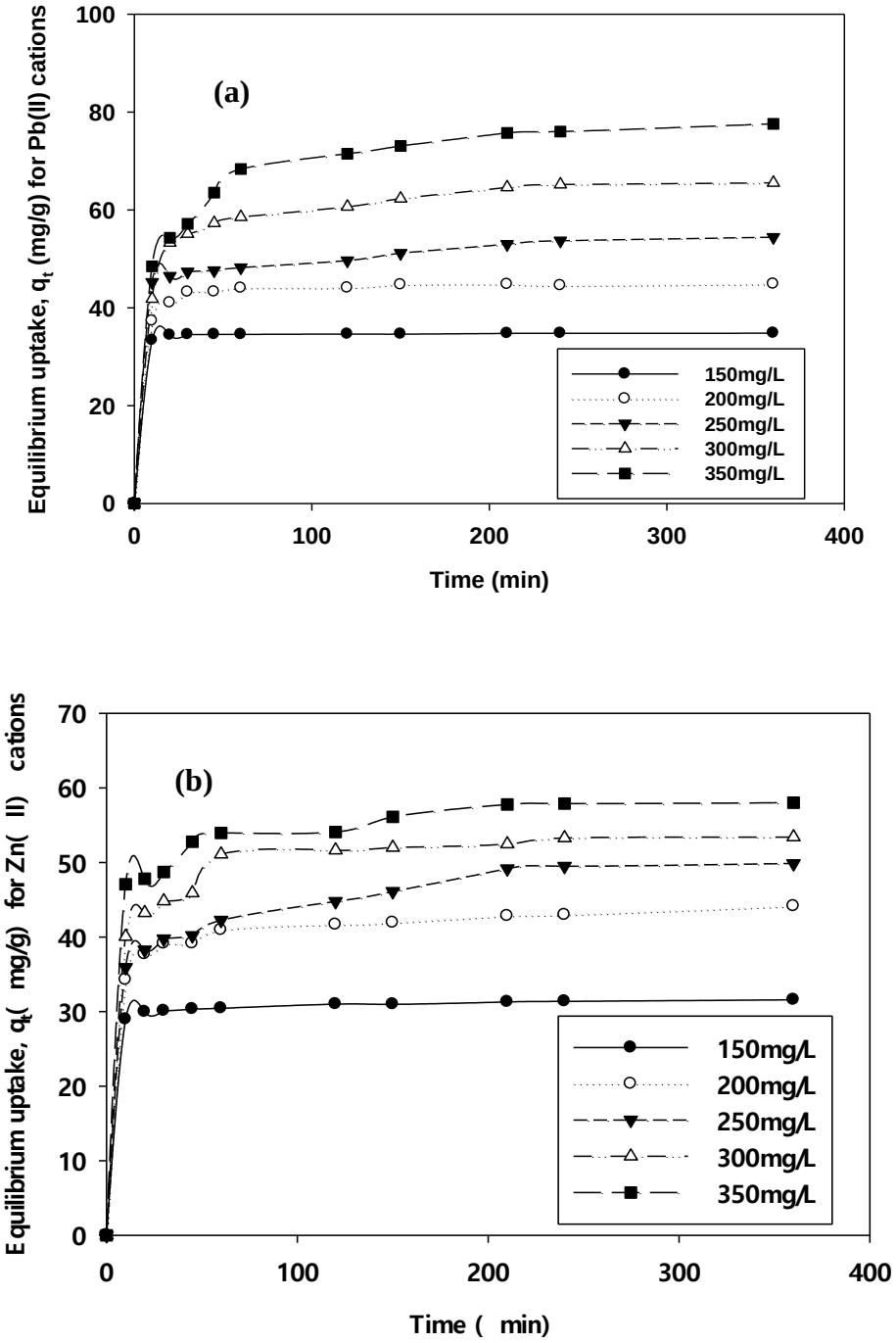

Fig. 2. Effect of (a) initial Pb(II) ion concentration and (b) initial Zn(II) ion concentration with contact time (C_o = 150 mg/L to 350mg/L) at temperature 30 °C and pH 5.5 for Rattan Sawdust Activated Carbon (RSAC)

Effect of pH

The solution pH has the ability to either suppress or uplift the adsorption capacity of an adsorbate, which is usually attributed to change of the activated carbon charge when the solution pH is altered (Nguyen *et al.* 2013). Increase in pH up to between 5 and 7.5 leads to availability of more negatively charged surface groups, thereby contributing

to more metal adsorption (Chigondo *et al.* 2013). The surface of an adsorbent is normally surrounded by the presence of hydroxonium ions (H^+) at lower pH values which usually block metal ions from binding onto adsorbents (Onundi *et al.* 2010).

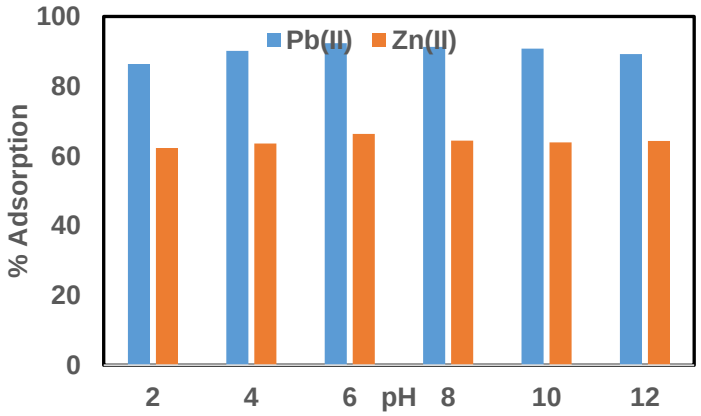

Fig. 3. Effect of pH on Percentage Adsorption

At pH lower than pH 4, there will be serious competition between the concentration of H+ and H_3O^+ ions and M^{2+} cations present in solution which leads to reduced adsorption of the cations by the adsorbents. Thus the adsorptions of the metal ions under investigation are generally low at lower pH. Moreover, at pH slightly higher than 8, three different species of metal ions will be available in solution and will interact with the OH^- groups present. This will invariably lead to greater adsorption by either ion exchange and or hydrogen bonding mechanisms. Such similar trend has been reported (Nguyen *et al.* 2013)

Kinetics Studies

Adsorption kinetics models are usually employed to determine both the adsorption mechanism and the potential rate-controlling steps, such as mass transfer and chemical reaction that have taken place during the sorption process. The adsorption kinetics elucidates the adsorption uptake of the adsorbate, Pb(II) and Zn(II) ions, onto the adsorbent (activated carbon). As stated earlier, the pseudo first order, pseudo second order, and Elovich kinetic models were employed in this work to study the kinetics of the adsorption process. Furthermore, the intra-particle diffusion model was applied to determine the diffusion mechanism of the system being studied. Adsorption kinetics models are usually employed to determine both the adsorption mechanism and the potential rate controlling steps, such as mass transfer and chemical reaction that have taken place during the sorption process. The adsorption kinetics elucidates the adsorption uptake of the adsorbates, Pb(II) and Zn(II) ions, onto the adsorbent (activated carbon). For all the models, the kinetic data obtained were analyzed using Sigma Plot, version 10.

The pseudo first order kinetic model has been used extensively to envisage the sorption kinetics (Srivastava and Hasan 2011). The linear form of the model can be expressed by the following Eqs. (9) and (10),

$$\log(q_e - q_t) = \log q_e - \frac{K_1}{2.303} t \quad (9)$$

$$h = K_1 q_{e_{cal}} \quad (10)$$

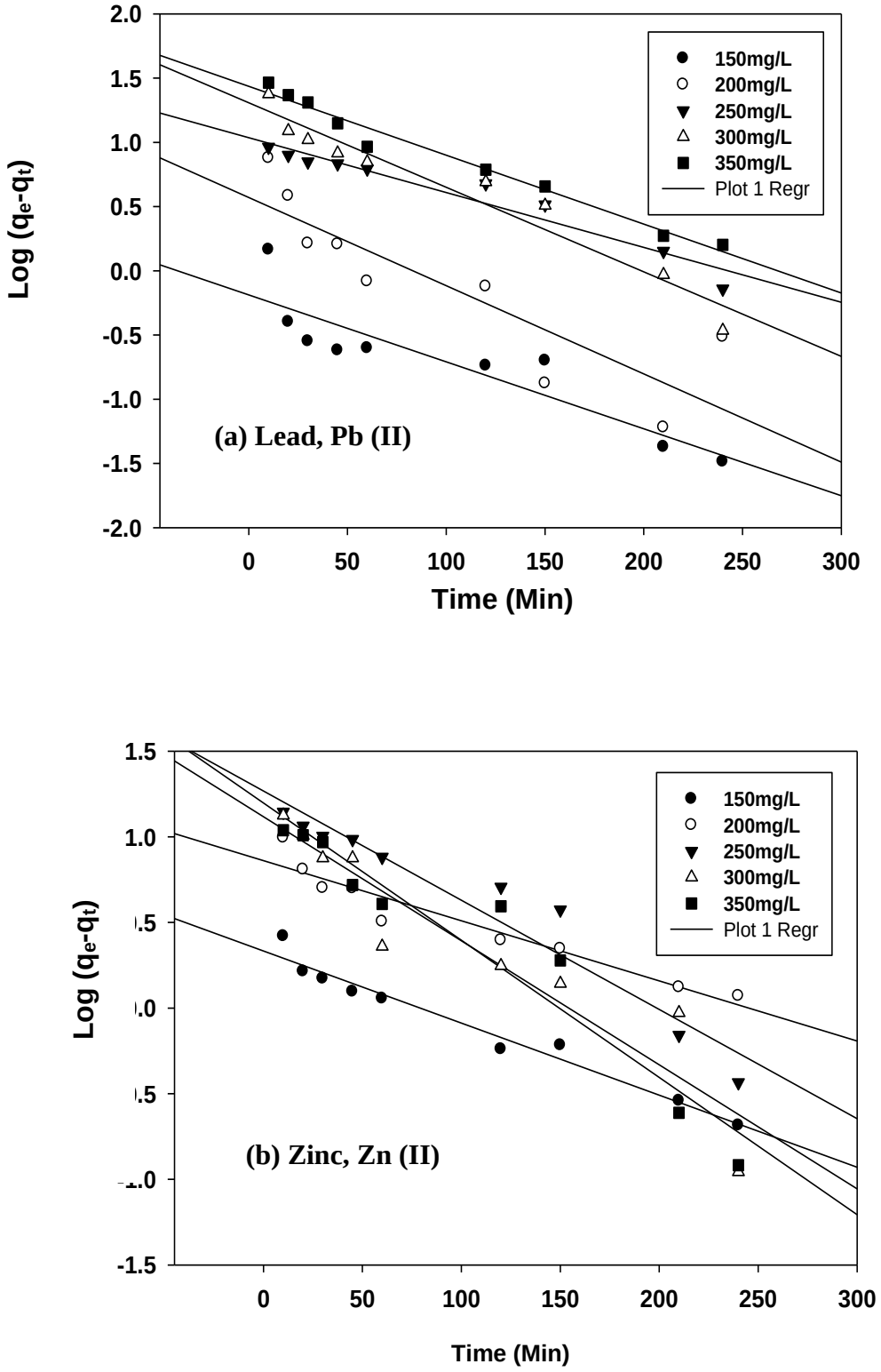

Fig. 4. Pseudo first order kinetics plots for (a) Pb(II) and (b) Zn(II) cations onto RSAC (initial concentration C_o = 150 mg/L – 350 mg/L at 30 ^oC and pH 5.5)

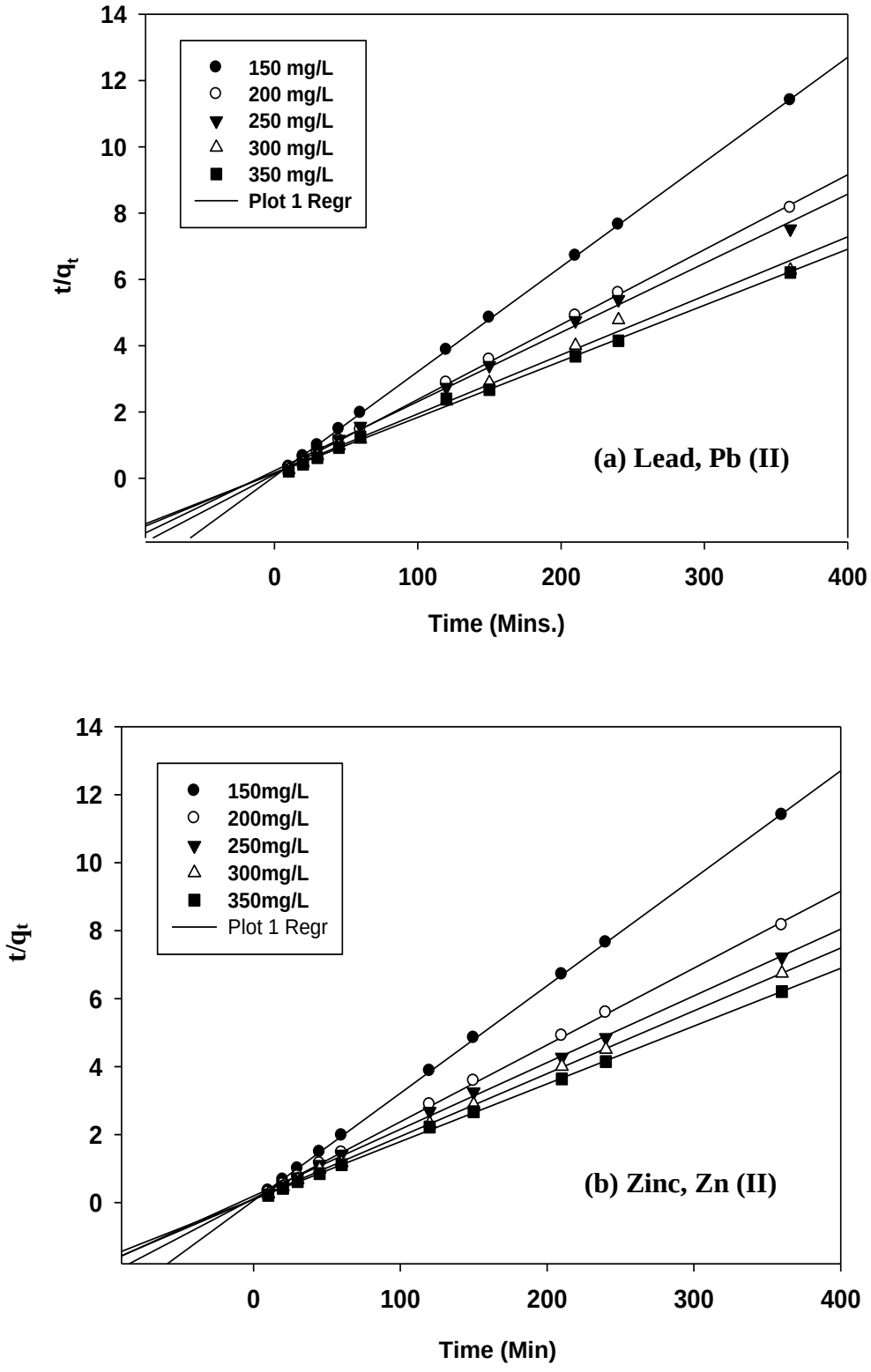

Fig. 5. Pseudo second order kinetics plots for (a) Pb(II) and (b) Zn(II) cations onto RSAC (initial concentration C_o = 150 mg/L – 350 mg/L at 30 ^oC and pH 5.5)

Table 5. Pseudo First Order and Pseudo Second Order Model Constants, Coefficients of Determination, and Normalized Standard Deviation Values for Adsorption of Pb (II) And Zn (II) Cations onto RSAC At 30 °C

			Pseudo First Order					Pseudo Second Order				
Adsorbate	Initial Concentration Co (mg/L)	Removal %	q_e, exp (mg/g)	q_e, cal (mg/g)	K_1 (1/h)	R^2	Δq_t (%)	q_e, exp (mg/g)	q_e, cal (mg/g)	K_2 (g/mg h)	R^2	Δq_t (%)
	150	93.2	34.86	0.43	0.01	0.82	98.77	34.86	34.84	0.06	0.99	0.06
Pb (II)	200	89.6	44.78	1.77	0.02	0.76	96.05	44.78	45.05	0.01	0.99	0.59
	250	84.96	52.99	2.82	0.01	0.94	94.68	52.99	54.35	0.001	0.97	2.49
	300	86.71	64.60	3.70	0.02	0.94	94.28	64.60	66.67	0.002	0.99	3.10
	350	86.27	75.72	4.75	0.01	0.94	93.73	75.72	81.97	0.001	0.98	7.62
	150	82.67	30.97	1.40	0.01	0.97	95.50	30.97	31.65	0.02	0.98	2.14
Zn (II)	200	84	41.92	2.37	0.01	0.93	94.36	41.92	44.25	0.004	0.99	5.27
	250	70.64	44.11	3.11	0.01	0.89	92.94	44.11	47.85	0.002	0.99	7.82
	300	69.43	52.00	3.02	0.004	0.60	94.18	52.00	56.18	0.002	0.99	7.45
	350	64.26	56.11	3.65	0.02	0.84	93.50	56.11	59.17	0.002	0.99	5.17

where q_e and q_t are the amounts of adsorbate adsorbed (mg/g) at equilibrium and at time t (min), respectively, h (mg/g-min) is the initial rate of sorption, and K_1 (l/min) is the adsorption rate constant. Figure 4 (a and b) graphically represents the pseudo first order kinetics models for the adsorption of Pb(II) and Zn(II) ions from their aqueous solutions. The first order rate constant, K_1, and the theoretical uptake, q_e (mg/g), were calculated from the slope and intercepts of the linear plots of ln (q_e-q_t) *versus* t (min) for all the concentration range being studied here. The results obtained are listed in Table 5.

Unlike the pseudo first order model, the pseudo second order model determines the behavior of the adsorption process over a wide range of adsorptions (Chowdhury *et al*. 2012b). Overall, the model equations are represented by,

$$\frac{t}{q_t} = \frac{1}{k_2 q_e^2} + \frac{1}{q_e} t \quad (11)$$

$$h = K_2 q_{cal}^2 \quad (12)$$

where K_2 (g/mg-h) and h (mg/g-min) denote the rate constant of pseudo second order adsorption and the initial rate of sorption, respectively (Ho 2006). The linear plots of pseudo second order kinetics for Pb(II) and Zn(II) cations are illustrated by Fig. 5, (a) and (b), respectively. The rate constants for the second order kinetics and the initial sorption rate were calculated from these linear plots (Fig. 5, a and b) and are listed in Table 5.

For the pseudo second order model, the values of equilibrium uptake, $q_{e,exp}$ (mg/g), agreed almost precisely with calculated $q_{e,cal}$ (mg/g) for both the cations, which resulted in relatively low Δq_t. Apart from this, the R^2 (coefficient of determination) values obtained were nearly equal for both the cations, reflecting the better applicability of this model reflecting chemisorption nature of adsorption (Chowdhury *et al.* 2012a, b). As noticed from the pseudo first order model, there was a large difference between the $q_{e,exp}$ (mg/g) and $q_{e,cal}$ (mg/g) values, thereby resulting in larger Δq_t values compared to the pseudo second order kinetics.

The results obtained for the pseudo second order model agreed satisfactorily with the previous research carried out on the adsorption of Pb(II) and Zn(II) ions onto activated carbons synthesized from watermelon shell and walnut shell (Moreno-Barbosa *et al.* 2013), *Penicillium simplicissimum* (Fan *et al.* 2008), and low-cost adsorbents (Mishra and Patel 2009), jute stalk based carbon (Chowdhury *et al.* 2016) and fruit peel of mangosteen (Abd Hamid *et al.* 2014), where the adsorption processes were all best described by the pseudo second order kinetic model.

It could also be observed from Table 5 that the removal percentages of Pb(II) ions for all the initial concentrations by RSAC were higher than those obtained for Zn(II) ions. The reason for the higher adsorption of the Pb^{2+} ion might be due to its ionic potential, electronegativity, and softness parameters. Lead has an electronegativity of 2.33, while zinc has an electronegativity of 1.65 (Kalmykova *et al.* 2008). Since the electronegativity of lead is higher, its adsorption capacity should be greater (Depci *et al*. 2012). This result was in agreement with those obtained for watermelon shell and walnut shell (Moreno-Barbosa *et al.* 2013). The lower adsorption of zinc, especially by acid-activated carbon, could also be attributed to its completely filled d-orbital (d-10). Lead is a borderline soft cation, and it is expected to be adsorbed not only with the surface functional groups but also the basal plane (Adil 2006).

The experimental data obtained were fitted with an intra-particle diffusion equation model so as to describe the diffusion mechanism of the sorbate onto the interior of the sorbent. In the sorption process, intra-particle diffusion is used to examine the role of diffusion as the rate controlling step (Chowdhury *et al.* 2012b). It is usually a general expectation that during the adsorption process, uptake should vary proportionally with the square root of time ($t^{1/2}$) but not with contact time (t). The intra-particle diffusion model is normally referred to as the Weber and Morris (1962) model and is usually represented by the following equation (Kalavathy *et al.* 2005),

$$q_t = K_{id} t^{0.5} \quad (13)$$

where K_{id} (mg/g-h) is the intra-particle diffusion rate constant and can be obtained from the slope of the linear curve of q_t *versus* $t^{1/2}$, and C provides information about the thickness of the boundary layer. The larger the intercept, the greater is the boundary layer effect (Kannan and Sundaram 2001). The plot of q_t *versus* $t^{1/2}$ must be linear and must pass through the origin for particle diffusion to be involved in the rate-limiting step. Otherwise, some other rate-limiting mechanisms may have been involved (Mall *et al.* 2006). The plots of q_t *versus* $t^{1/2}$ for both the cations were linear, but they did not pass through the origin. This suggested that the intra-particle diffusion was not the only rate-controlling step involved in the adsorption process (Fig. 6). Table 6 lists the intra-particle diffusion constants and the coefficients of determination for the adsorption of Pb(II) and Zn(II) cations onto RSAC.

Table 6. Intra-particle Diffusion Model Constants, Coefficients of Determination, and Normalized Standard Deviation Values for Adsorption of Pb(II) and Zn(II) Cations onto RSAC at 30 ºC

Adsorbate	Initial Concentration C_o (mg/L)	Final Concentration C_e (mg/L)	Removal (%)	K_{id}	C_1	R^2
Pb(II)	150	10.2	93.2	0.05	33.95	0.47
	200	20.8	89.6	0.33	39.84	0.56
	250	37.6	84.96	0.60	43.65	0.98
	300	41.2	86.71	1.20	46.48	0.76
	350	46.5	86.27	2.78	34.96	0.65
Zn(II)	150	26	82.67	0.14	29.17	0.88
	200	32	84	0.51	35.33	0.84
	250	73.4	70.64	0.92	31.30	0.94
	300	91.7	69.43	0.90	39.94	0.82
	350	125.1	64.26	0.83	43.67	0.88

(a) Lead, Pb(II)

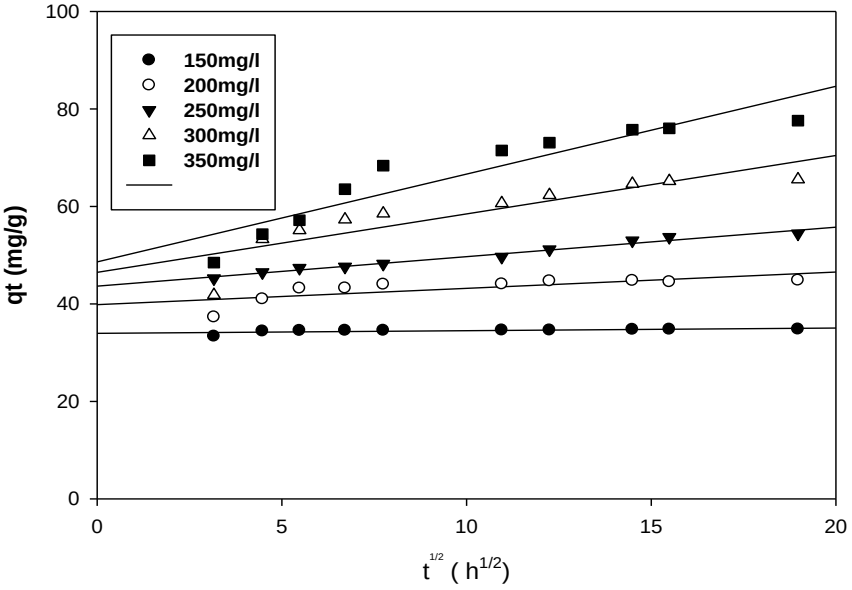

(b) Zinc, Zn(II)

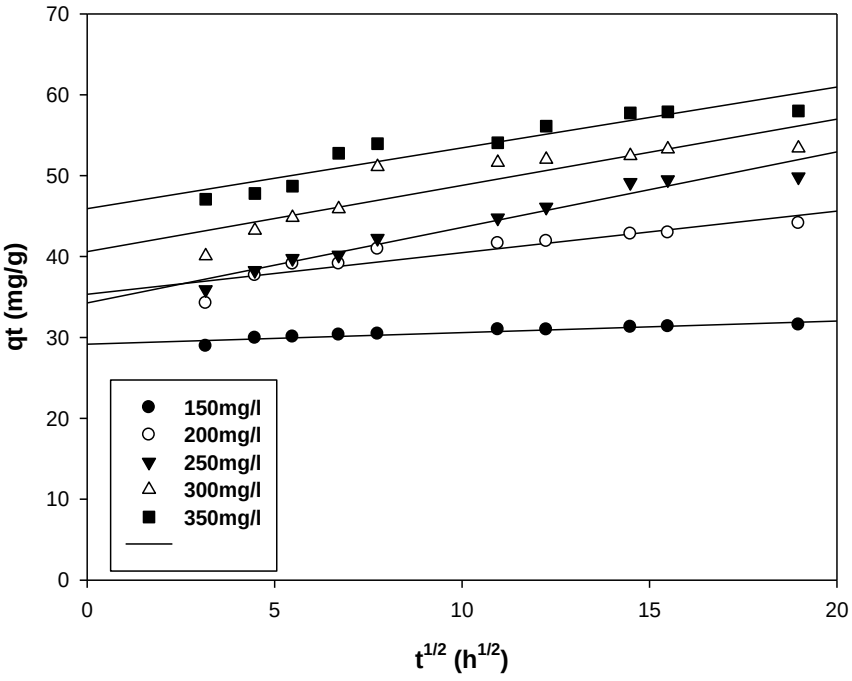

Fig. 6. Intra-particle diffusion plots for (a) Pb(II) and (b) Zn(II) cations onto RSAC (initial concentration C_o = 150 mg/L – 350 mg/L at 30 ºC and pH 5.5)

The Elovich equation was also found to successfully define the second order kinetics, assuming that the actual solid surfaces are actively heterogeneous, but the equation does not suggest a specific mechanism for the adsorbate-adsorbent system (Yakout and Elsherif 2010).

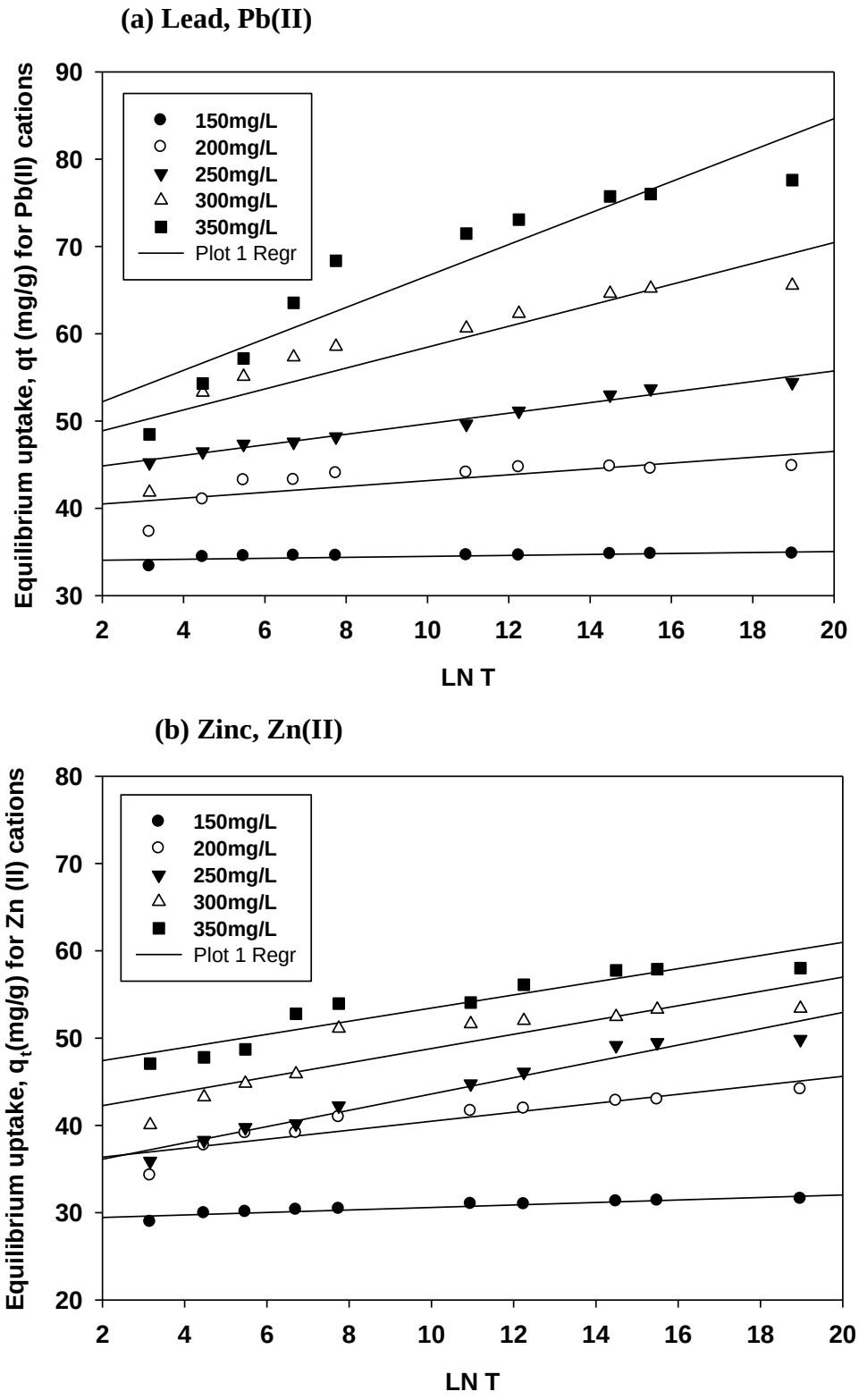

Fig. 7. Elovich model plots for (a) Pb (II) and (b) Zn (II) cations onto RSAC (initial concentration C_o = 150 mg/L – 350 mg/L at 30 ^oC and pH 5.5)

Table 7. Elovich Model Constants, Coefficients of Determination, and Normalized Standard Deviation Values for Adsorption of Pb(II) and Zn(II) Cations onto RSAC at 30 °C

Adsorbate	Initial Concentration C_o (mg/L)	Final Concentration C_e (mg/L)	Removal (%)	q_e, exp (mg/g)	q_e, cal (mg/g)	(1/*b*)ln*ab* (mg/g)	1/b (mg/g)	R^2	∆qt (%)
Pb(II)	150	10.2	93.2	34.86	33.51	33.27	0.29	0.64	3.87
	200	20.8	89.6	44.78	40.58	35.68	1.74	0.75	9.37
	250	37.6	84.96	52.99	50.38	38.24	2.65	0.94	4.93
	300	41.2	86.71	64.60	60.17	33.32	5.82	0.91	6.86
	350	46.5	86.27	75.72	80.07	2.18	14.03	0.83	5.43
Zn(II)	150	26	82.67	30.97	31.49	24.70	0.67	0.97	1.65
	200	32	84	41.92	40.41	29.92	2.44	0.95	3.60
	250	73.4	70.64	44.11	40.24	22.51	4.17	0.97	8.77
	300	91.7	69.43	52.00	50.24	30.95	4.16	0.89	3.38
	350	125.1	64.26	56.11	50.28	36.65	3.55	0.80	10.39

The chemisorption process can be described well by the following semi-empirical equation (Yakout and Elsherif 2014). The linear form of this equation is given by,

$$q_t = \frac{1}{b} Ln(ab) + \frac{1}{b} Lnt \quad (14)$$

where *a* (mg/g-h) represents the initial sorption rate, and *b* (g/mg) reflects the activation energy required to exhibit the extent of surface coverage for chemisorption. The value of 1/*b* ln (*ab*) is the sorption quantity when the logarithm of *t* (time) equals to zero, that is, when *t* is 1 hour, whereas 1/*b* indicates the number of sorption sites available for binding. The linear plots of the Elovich model are shown in Fig. 7, and the model parameters are listed in Table 7. The good linearity of the curve, as illustrated by Fig. 7, and the high coefficients of determination with small deviation percentages further support the chemisorption nature of the adsorption process.

Thermodynamic Characterization

In the study of the thermodynamics, parameters such as the enthalpy change (ΔH^o), entropy change (ΔS^o), and change in Gibbs free energy (ΔG^o) were evaluated. These parameters are related to the coefficient of distribution of the solute between the solid and the liquid phases during the adsorption process. The thermodynamic parameters were obtained from the plots of ln K_L *versus* 1/*T*, where K_L is the Langmuir constant obtained earlier at the temperatures of 303 °K, 333 °K and 353 °K, and *T* is the absolute temperature in Kelvin. By applying the following equation, the thermodynamic values were obtained (Chowdhury *et al.* 2012b),

$$\ln \mathrm{K}_L = \frac{S}{\mathrm{R}} - \frac{H}{\mathrm{RT}} \quad (15)$$

$$G = \mathrm{R}TLn\mathrm{K}_\mathrm{L} \quad (16)$$

where the constant, K_L, was determined from the Langmuir equation at three different temperatures (L/mg; Table 11), *R* is the universal gas constant (8.314 J/mol·K), and *T* is the absolute temperature (K).

The thermodynamic parameters of Gibbs free energy ($\Delta G°$), enthalpy ($\Delta H°$), and entropy ($\Delta S°$) were estimated and are provided in Table 8. After subjecting the experimental data to thermodynamic evaluation, the results obtained showed that the standard enthalpy change (ΔH^o) and the standard entropy change (ΔS^o) values were 0.1297 KJmol^{-1} and 0.5738 JK^{-1}mol^{-1} for Pb(II) cations and 0.123 KJmol^{-1} and 2.7644 JK^{-1}mol^{-1} for Zn(II) cations, respectively. These positive values for enthalpy change ($\Delta H°$) indicated that the adsorption process was endothermic in nature (Abd Hamid *et al.* 2014). Moreover, the adsorption uptake of both the cations increased with the increase in temperature. The positive value of entropy change (ΔS^0) revealed the good affinity of Pb(II) and Zn(II) ions towards the sorbent and the increasing randomness at the solid-solution interface during the adsorption process (Yakout and Elsherif 2010; Chowdhury *et al.* 2011a,b). The negative values obtained for the standard free Gibb's Free Energy ($\Delta G°$) was an indication that the process of adsorption was spontaneous and could feasibly take place. Similar phenomena were reported in our previous work on the removal of the divalent cations Pb(II) and Zn(II) onto banana empty fruit bunch-based activated carbon (Adebesi *et al*. 2016).

Table 8. Thermodynamic Parameters of Pb(II) and Zn(II) Sorption by RSCAC

Pollutant	Temperature (K)	Thermodynamic Parameters			
		$\Delta G°$ (kJ·mol^{-1})	$\Delta H°$ (kJ·mol^{-1})	$\Delta S°$ (J·K^{-1}·mol^{-1})	R^2
	303	-7.963			
Pb(II)	333	-3.696	0.130	0.514	0.997
	353	-3.771			
	303	-8.996			
Zn(II)	333	-8.357	0.123	2.764	0.999
	353	-9.302			

Desorption Studies

The feasibility of the prepared adsorbent was further analyzed using five types of chemical regenerating agent. The regeneration of spent activated carbon can be done either by using either thermal or chemical regeneration methods. The use of thermal regeneration usually requires a high amount of energy, which also leads to the loss of adsorbent (Rao *et al.* 2006). It was observed that the percent desorption was higher for Zn(II) cations than for Pb(II) cations. This might be due to the smaller cationic size of Zn(II) (0.74 °A) compared to Pb(II) (1.19 °A). However, a satisfactory desorption percentage was exhibited by the prepared carbon sample using 1 M HNO_3 (Table 9). A similar desorption efficiency had also been observed for Cd(II) and Zn(II) cations from rice husk ash when using an acid eluting agent (Srivastava *et al.* 2008).

Table 9. Percent Desorption of Pb(II) and Zn(II) Cations from Spent Activated Adsorbent (RSCAC)

Adsorbate	Desorption Percentages				
	Distilled Water	CH_3COOH	HCl	HNO_3	H_2SO_4
Pb (II)	15.89	21.33	64.77	86.87	32.54
Zn (II)	25.88	24.09	69.98	92.88	39.89

The sorption process takes place either by physical or chemical interactions, ion exchange or a combination of all types of mechanisms. By using distilled water, small fractions of cations can be desorbed. Mineral acids are better than organic acids as desorbing agents. Basically, organic acids dissociate partially, releasing smaller amounts of exchangeable H^+ ions. On the contrary, inorganic acids dissociate completely and thus produce a sufficient number of H^+ cations (Chowdhury 2013). These take part in the desorption mechanisms of metallic cations from the adsorbent surface. H_2SO_4 could not desorb significant amount of metallic cation due to formation of insoluble SO_4^{-2} ions which was precipitated and blocking the pores. Among the inorganic acids, HNO_3 acid acts as better eluting agent for activated carbon. Overall, the HNO_3 desorption technique was shown to be a promising way to regenerate both the cation loaded sorbents.

CONCLUSIONS

1. The two-step activation technique that was used to prepare the carbon (RSCAC) from *Calamus gracilis* sawdust was successful at creating adequate porocities with enhanced surface area for the adsorption of Pb (II) and Zn (II) cations from synthetic waste water.
2. The adsorption of both the cations onto the RSCAC followed the Lanumuir and Freundlich models more than the Temkin adsorption isotherm model for all the temperatures studied here.
3. The adsorption proceeded according to the pseudo-second-order and Elovich models, which provided the best correlations within the data in all cases, such that the experimental q_e(exp) values agreed with the calculated ones. Also, it was observed that the intra-particle diffusion was not the only rate-controlling step.
4. Equilibrium uptake increased with the increase in temperature, reflecting the endothermic nature of the sorption, which was further confirmed by the thermodynamic charecterizations of the system. The positive $\Delta H°$ and $\Delta S°$ values indicated that the adsorption of PB(II) and Zn(II) cations onto the RSCAC was endothermic and that the ions had a good affinity towards the sorbent. The adsorbed cations for both the metal ions could be effectively eluted using 1 M HNO_3 acid with the desorption efficiencies of 86.87 and 92.88% for Pb(II) and Zn(II), respectively. Thus, it could be concluded that the hydrochar-based carbon (RSCAC) could be used efficiently, reflecting its feasibility for commercial application.

ACKNOWLEDGMENTS

The authors thank the University of Malaya for financial support (BK054-2015).

REFERENCES CITED

Abdel-Halim, S., Shehata, A., and El-Shahat, M. (2003). "Removal of lead ions from industrial waste water by different types of natural materials," *Water Research* 37(7), 1678-1683. DOI: 10.1016/S0043-1354(02)00554-7

Abd Hamid, S. B., Chowdhury, Z. Z., and Zain, S. M. (2014). "Base catalytic approach: A promising technique for activation of bio char for equilibrium sorption studies of copper, Cu (II) ions in single solute system," *Materials* 7(4), 2815-2832. DOI: 10.3390/ma7042815

Adebisi, G. A., Chowdhury, Z. Z., Abd Hamid, S. B., and Ali, E. (2016). "Hydrothermally-treated banana empty fruit bunch fiber activated carbon for Pb(II) and Zn(II) removal," *BioResources* 11(4), 9686-9709. DOI: 10.15376/biores.11.4. 9686-9709

Adil, M. (2006). "Preparation, modification and characterization of activated carbons for batch adsorption studies on the removal of selected metal ions," M.Sc Thesis, University Technology, Malaysia.

Al-Othman, Z., Habila, M., and Ali, R. (2011). "Preparation of activated carbon using the co-pyrolysis of agricultural and municipal solid wastes at a low carbonization temperature," *Carbon* 20, 21.

Amaya, A., Medero, N., Tancredi, N. H., Silva, H., and Deiana, C. (2007). "Activated carbon briquettes from biomass materials," *Bioresour. Technol.* 98(8), 1635-1641. DOI: 10.1016/j.biortech.2006.05.049

Amuda, O., Giwa, A., and Bello, I. (2007). "Removal of heavy metal from industrial wastewater using modified activated coconut shell carbon," *Biochemical Engineering Journal* 36(2), 174-181. DOI: 10.1016/j.bej.2007.02.013

Baccar, R., Bouzid, J., Feki, M., and Montiel, A. (2009). "Preparation of activated carbon from Tunisian olive-waste cakes and its application for adsorption of heavy metal ions," *Journal of Hazardous Materials* 162(2), 1522-1529. DOI: 10.1016/j.jhazmat.2008.06.041

Bulut, Y., and Tez, Z. (2007). "Removal of heavy metals from aqueous solution by sawdust adsorption," *Journal of Environmental Science* 19, 160-166. DOI: 10.1016/S1001-0742(07)60026-6

Chowdhury, Z. Z., Zain, S. M., and Rashid, A. K. (2011a). "Equilibrium isotherm modeling, kinetics, and thermodynamics study for removal of lead from waste water," *E- Journal of Chemistry* 8(1), 333- 339. DOI: org/10.1155/2011/184040.

Chowdhury, Z. Z., Zain, S. M., Rashid, A. K., Ahmad, A. A., Islam, M. S., and Arami-Niya, A. (2011b). "Application of central composite design for preparation of kenaf fiber based activated carbon for adsorption of manganese (II) ion," *International Journal of Plant Sciences* 6(31), 7191-7202. DOI: 10.5897/IJPS11.1510.

Chowdhury, Z. Z., Zain, S. M., Khan, R. A., and Islam, M. S. (2012a). "Preparation and characterizations of activated carbon from kenaf fiber for equilibrium adsorption studies of copper from wastewater," *Korean Journal of Chemical Engineering* 29(9), 1187-1195. DOI: 10.1007/s11814-011-0297-9

Chowdhury, Z. Z., Zain, S. M., Khan, R. A., Rafique, R. F., and Khalid, K. (2012b). "Batch and fixed bed adsorption studies of lead (II) cations from aqueous solutions onto granular activated carbon derived from *Mangostana garcinia* shell," *BioResources* 7(3), 2895-2915. DOI: 10.15376/biores.7.3.2895-2915

Chowdhury, Z. Z., Hasan, M. D., Abd Hamid, S. B., Shamsudin, E. M., Zain, S. M., and Khalid, K. (2015). "Catalytic pretreatment of biochar residues derived from lignocellulosic feedstock for equilibrium studies of manganese, Mn (II) cations from aqueous solution," *RSC Advances* 5(9)**,** 6345-6356. DOI: 10.1039/C4RA09709B.

Chowdhury Z. Z., Abd. Hamid S. B., and Rafique, R. F. (2016). "Catalytic activation and application of micro-spherical carbon derived from hydrothermal carbonization of lignocellulosic biomass: Statistical analysis using Box-Behnken design," *RSC Advances* 6(104), 102680-102694.

Chowdhury, Z. Z. (2013). "Preparation, characterization and adsorption studies of heavy metals onto activated adsorbent materials derived from agricultural residues," University Malaya, Malaysia.

Chigondo, F., Nyamunda, B., Sithole, S., and Gwatidzo, L. (2013). "Removal of lead (II) and copper (II) ions from aqueous solution by baobab (*Adononsia digitata*) fruit shells biomass," *IOSR Journal of Applied Chemistry* 5(1), 43-50.

Depci, T., Kul, A. R., and Önal, Y. (2012). "Competitive adsorption of lead and zinc from aqueous solution on activated carbon prepared from Van apple pulp: Study in single- and multi-solute systems," *Chemical Engineering Journal* 200, 224-236. DOI: 10.1016/j.cej.2012.06.077

Durán-Valle, C. J., Gómez-Corzo, M., Pastor-Villegas, J., and Gómez-Serrano, V. (2005). "Study of cherry stones as raw material in preparation of carbonaceous adsorbents," *Journal of Analytical and Applied Pyrolysis* 73(1), 59-67. DOI: 10.1016/j.jaap.2004.10.004

Ekebafe, L., Ekebafe, M., Erhuaga, G., and Oboigba, F. (2012). "Effect of reaction conditions on the uptake of selected heavy metals from aqueous media using composite from renewable materials," *American Journal of Polymer Science* 2(4), 67-72. DOI: 10.5923/j.ajps.20120204.04

Fan, T., Liu, Y., Feng, B., Zeng, G., Yang, C., Zhou, M., and Wang, X. (2008). "Biosorption of cadmium (II), zinc (II), and lead (II) by *Penicillium simplicissimum*: Isotherms, kinetics and thermodynamics," *Journal of Hazardous Materials* 160(2), 655-661. DOI: 10.1016/j.jhazmat.2008.03.038

Falco, C., Sieben, J. M., Brun, N., Sevilla, M., Van der Mauelen, T., Morallon, E., Cazorla-Amoros, D., and Titirici, M. M. (2013). "Hydrothermal carbons from hemicellulose-derived aqueous hydrolysis products as electrode materials for supercapacitors," *Chem. Sus. Chem.* 6(2), 374-382. DOI: 10.1002/cssc.201200817

Fernandez, M. E., Ledesma, B., Román, S., Bonelli, P. R., and Cukierman, A. L. (2015). "Development and characterization of activated hydrochars from orange peels as potential adsorbents for emerging organic contaminants," *Bioresource Technol*ogy 183(2015), 221-228. DOI: 10.1016/j.biortech.2015.02.035

Foo, K., and Hameed, B. (2011). "Preparation of oil palm (*Elaeis*) empty fruit bunch activated carbon by microwave-assisted KOH activation for the adsorption of methylene blue," *Desalination* 275(1), 302-305. DOI:10.1016/j.desal.2011.03.024

Freundlich, H. M. F. (1906). "Over the adsorption in solution," *Journal of Physical Chemistry* 57(1906), 385-471.

Gratuito, M. K. B., Panyathanmaporn, T., Chumnanklang, R.-A., Sirinuntawittaya, N., and Dutta, A. (2008). "Production of activated carbon from coconut shell: Optimization using response surface methodology," *Bioresource Technology* 99(11), 4887-4895. DOI: 10.1016/j.biortech.2007.09.042

Hao, W., Björkman, E., Lilliestråle, M., and Hedin, N., (2014). "Activated carbons for water treatment prepared by phosphoric acid activation of hydrothermally treated beer waste," *Ind. Eng. Chem. Res*. 53, 15389-15397, DOI:10.1021/ie5004569.

Hameed, B., Ahmad, A., and Latiff, K. (2007). "Adsorption of basic dye (methylene blue) onto activated carbon prepared from rattan sawdust," *Dyes and Pigments* 75(1), 143-149. DOI: 10.1016/j.dyepig.2006.05.039

Hawari, A., Rawajfih, Z., and Nsour, N. (2009). "Equilibrium and thermodynamic analysis of zinc ions adsorption by olive oil mill solid residues," *Journal of Hazardous Materials* 168(2), 1284-1289. DOI: 10.1016/j.jhazmat.2009.03.014

Ho, Y. S. (2006). "Review of second order models for adsorption systems," *Journal of Hazardous Materials* 136, 681-689.

Kannan, N., and Sundaram, M. M. (2001). "Kinetics and mechanism of removal of methylene blue by adsorption on various carbons—A comparative study," *Dyes and Pigments* 51(1), 25-40. DOI: 10.1016/S0143-7208(01)00056-0

Kalmykova, Y., Strömvall, A.-M., and Steenari, B.-M. (2008). "Adsorption of Cd, Cu, Ni, Pb and Zn on Sphagnum peat from solutions with low metal concentrations," *Journal of Hazardous Materials* 152(2), 885-891. DOI: 10.1016/j.jhazmat.2007.07.062

Kalavathy, M. H., Karthikeyan, T., Rajgopal, S., and Miranda, L. R. (2005). "Kinetic and isotherm studies of Cu (II) adsorption onto H_3PO_4-activated rubber wood sawdust," *Journal of Colloid and Interface Science* 292, 354-362.

Khezami, L., Bessadok-Jemai, A., Al-Dauij, O., and Amami, E. (2012). "Individual and competitive adsorption of Lead (II) and Nickel (II) ions by chemically activated carbons," *International Journal of Plant Sciences* 7, 6075-6081.

Langmuir, I. (1918). "The adsorption of gases on plane surfaces of glass, mica and platinum," *Journal of American Chemical Society* 40(9), 1361-1403. DOI: 10.1021/ja02242a004

Liu, F., and Guo, M. (2015). "Comparison of the characteristics of hydrothermal carbons derived from holocellulose and crude biomass," *Journal of Material Science* 50(4), 1624-1631. DOI: 10.1007/s10853-014-8723-0

Mall, I. D., Srivastava, V. C., Kumar, G. V. A., and Mishra, I. M. (2006). "Characterization and utilization of mesoporous fertilizer plant waste carbon for adsorptive removal of dyes from aqueous solution," *Colloids and Surfaces A.* 278, 175-187.

Moreno-Barbosa, J. J., López-Velandia, C., del Pilar Maldonado, A., Giraldo, L., and Moreno-Piraján, J. C. (2013). "Removal of lead (II) and zinc (II) ions from aqueous solutions by adsorption onto activated carbon synthesized from watermelon shell and walnut shell," *Adsorption* 19(2-4), 675-685. DOI: 10.1007/s10450-013-9491-x

Nguyen, T., Ngo, H., Guo, W., Zhang, J., Liang, S., Yue, Q. Y., Li, Q., and Nguyen, T. (2013). "Applicability of agricultural waste and by-products for adsorptive removal of heavy metals from wastewater," *Bioresource Technology* 148, 574-585. DOI: 10.1016/j.biortech.2013.08.124.

Onundi, Y. B., Mamun, A., Al Khatib, M., and Ahmed, Y. M. (2010). "Adsorption of copper, nickel and lead ions from synthetic semiconductor industrial wastewater by palm shell activated carbon," *International Journal of Environmental Science & Technology* 7(4), 751-758. DOI:10.1007/BF03326184

Rao, M. M., Ramesh, A., Rao, G. P. C., and Seshaiah, K. (2006). "Removal of copper and cadmium from the aqueous solutions by activated carbon derived from *Ceiba pentandra* hulls," *Journal of Hazardous Materials* 129(1), 123-129. DOI: 10.1016/j.jhazmat.2005.08.018

Saqib, U. N., Oh, M., Jo, W., Park, S., and Lee, J.-Y. (2015). "Conversion of dry leaves into hydrochar through hydrothermal carbonization (HTC)," *Journal of Material Cycles and Waste Management* (online). DOI: 10.1007/s10163-015-0371-1

Sevilla, M., and Fuertes, A. B. (2009). "The production of carbon materials by hydrothermal carbonization of cellulose," *Carbon* 47(9), 2281-2289. DOI: 10.1016/j.carbon.2009.04.026

Srivastava, P., and Hasan, S. H. (2011). "Biomass of mucor heimalis for the biosorption of cadmium from aqueous solutions: Equilibrium and kinetics study," *BioResources* 6(4), 3656-3675. DOI: 10.15376/biores.6.4.3656-3675

Srivastava, V. C., Mall, I. D., and Mishra, I. M. (2008). "Removal of cadmium and zinc metal ions from binary aqueous solution by rice husk ash," *Colloids and Surfaces A: Physicochemical and Engineering Aspects* 312, 172-184.

Titirici, M. M., Antonietti, M., and Baccile, N. (2008). "Hydrothermal carbon from biomass: A comparison of the local structure from poly- to monosaccharides and pentoses/hexoses," *Green Chem*. 10(11), 1204-1212. DOI: 10.1039/B807009A

Temkin, M. J., and Pyzhev, V. (1940). "Recent modification to Langmuir isotherms," *Acta Physical Chemistry* 12, 217-225.

Vernersson, T., Bonelli, P., Cerrella, E., and Cukierman, A. (2002). "*Arundo donax* cane as a precursor for activated carbons preparation by phosphoric acid activation," *Bioresource Technology* 83(2), 95-104. DOI: 10.1016/S0960-8524 (01) 00205-X

Wang, Y., Qiao, M., Liu, Y., and Zhu, Y. (2012). "Health risk assessment of heavy metals in soils and vegetables from wastewater irrigated area, Beijing-Tianjin city cluster, China," *Journal of Environmental Sciences* 24(4), 690-698. DOI: 10.1016/S1001-0742(11)60833-4

Yakout, S. M., and Elsherif, E. (2010). "Batch kinetics, isotherm and thermodynamic studies of adsorption of strontium from aqueous solutions onto low cost rice-straw based carbons," *Carbon – Science and Technology* 1, 144-153.

Zhang, K., Cheung, W., and Valix, M. (2005). "Roles of physical and chemical properties of activated carbon in the adsorption of lead ions," *Chemosphere* 60(8), 1129-1140. DOI: 10.1016/j.chemosphere.2004.12.059

Article submitted: June 13, 2016; Peer review completed: September 4, 2016; Revised version received: January 19, 2017; Second revised version received and accepted: January 21, 2017; Published: February 28, 2017.
DOI: 10.15376/biores.12.2.2872-2898